Available online at www.eccomasproceedia.org
Eccomas Proceedia COMPDYN (2025) 4409-4419

ECCOMAS
Proceedia

COMPDYN 2025
10th ECCOMAS Thematic Conference on
Computational Methods in Structural Dynamics and Earthquake Engineering
M. Papadrakakis, M. Fragiadakis (eds.)
Rhodes Island, Greece, 15-18 June 2025

EFFECT OF INPUT MOTION SELECTION STRATEGY ON THE ASSESSMENT OF SEISMIC PERFORMANCE OF BRIDGES

I. MIKES[1], A. KAPPOS[1], E. RIGA[2], T. KISHIDA[1]

[1] Department of Civil and Environmental Engineering, Khalifa University of Science & Technology, Abu Dhabi, UAE

[2] Department of Civil Engineering, Aristotle University of Thessaloniki, Thessaloniki, Greece

Abstract

Despite being the reference method in most modern seismic codes and broadly used in research, until recently nonlinear response history analysis (NLRHA) has been employed by practising engineers to a very limited extent. Two reasons that NLRHA has recently become a more feasible option are the introduction of detailed code provisions for its application and the development of open-access strong motion databases that enable the automated selection of ground motion. In the absence of a broader consensus on criteria for ground motion selection, modern seismic codes have historically recommended using the code-prescribed design spectrum (CDS) or the uniform hazard spectrum (UHS) as target spectra over a specific period range. However, both CDS and UHS are considered generally conservative. Alternatively, recent codes, such as ASCE 7 and the upcoming second-generation Eurocode 8, offer the option of using the conditional mean spectrum (CMS), where the spectral acceleration (S_a) at a period of interest is picked from the UHS and the other S_a values are correlated to it. In this paper, different ground motion sets are selected based on all commonly used approaches, i.e. CDS, UHS, CMS, and a new one based on CMS conditioned at multiple periods (CMSV), utilising an in-house developed software tool. The effect of selection method on the resulting sets of ground motions, as well as the effect of ground motion selection on the seismic assessment of bridges are then examined by subjecting a typical modern bridge to NLRHA using alternative sets of ground motions.

Keywords: input motion selection; second-generation Eurocode 8; disaggregation; uniform hazard spectrum; conditional mean spectrum; bridges; recorded ground motions

ISSN:2623-3347
Peer-review under responsibility of the organizing committee of COMPDYN 2025.
doi: 10.7712/120125.12745.2599

1 INTRODUCTION

The appropriate selection of ground motions is one of the most challenging parts for the structural engineer when assessment or design is done by employing nonlinear response history analysis (NLRHA). Despite the increasing availability of open-access databases and software that facilitates the procedure of recorded ground motion selection, such as the NGA-West2 [1] with its search filters and spectrum-matching criteria or the Pan-European Engineering Strong Motion (ESM) database and its integrated selection tool REXELweb [2], the relative scarcity of the particularly important large-magnitude and near-source records is one key obstacle in the procedure of ground motion selection when matching a target spectrum is sought [3]. Constant-amplitude scaling of recorded motions to a target spectrum is usually deemed to be the solution to this problem in both the literature and seismic codes. Nevertheless, it is still a controversial method, and it has been suggested to avoid it if possible, since it may introduce bias in the seismic response estimation [4]. These limitations have led modern seismic codes to recommend minimum and maximum allowable ground motion scaling factors. An example is the upcoming Eurocode 8 – Part 1-1 [5], which restricts the allowable range of scaling factors between 0.5 and 2.0 in cases of highly nonlinear structural response or geotechnical applications.

The selection of the appropriate target spectrum is also a critical factor in the ground motion selection procedure, and it is known to have a substantial effect on the outcome of NLRHA. Traditionally, the code elastic design spectrum (CDS), which is a generalised, smoothened version of the uniform hazard spectrum (UHS), has been used as the target for ground motion selection and scaling. However, CDS and UHS generally lead to a significant overestimation of the NLRHA results which led to the development of more realistic spectra that have already been adopted by several modern seismic codes, such as the Conditional Mean Spectrum (CMS) [6] or its Conditional Spectrum (CS) extension that accounts for the variability of the target response spectrum by incorporating the conditional standard deviation at each period [7]. As CMS is 'anchored' to a single conditioning period (T*), it is suitable for structures dominated by a single mode. A solution to overcome this limitation is the CMSV [8], which allows for conditioning on more than one or even a range of periods.

Another code requirement that often hinders motion selection is the relatively extensive period range over which matching with the target spectrum is needed, for instance $0.2T_1 – 1.5T_1$ [9]. This range is too broad, since the period elongation in typical frame structures has been reported to be less than 30% even when seismic actions exceeding two times the intensity of the design earthquake are applied [10], while in many regions, the lower bound of $0.2T_1$ often falls near the peak of a typical UHS. Similar selection criteria are used in most modern seismic codes, with the exception of the New Zealand code, which is less restrictive than the Eurocodes in terms of the required period range over which spectrum matching is checked [10].

Several theoretically sound solutions have been suggested to overcome these issues and facilitate the procedure of ground motion selection, including a) relaxation of the constraints on the causal rupture parameters, such as magnitude (M) and source-to-site distance (R), which have been used traditionally as ground motion selection criteria [11], b) spectral matching of ground motions to the target spectrum (e.g., [12]) and c) use of artificial or simulated ground motions. However, all of them have a number of drawbacks.

The main goal of this study is to assess the effect of the most common ground motion selection and scaling strategies on the calculated nonlinear response of bridges. For this purpose, a typical bridge is subjected to different sets of recorded ground motions, selected using different criteria and target spectra (CDS, UHS, CMS, CMSV), following the spectrum matching criteria of the new Eurocode 8 – Part 1-1. Records are selected from both the ESM

and NGA-West2 databases, using a computationally efficient 'greedy selection' algorithm, which is the first in the literature that is aligned with the requirements of the upcoming Eurocode 8.

2 SELECTION OF RECORDED GROUND MOTIONS BASED ON DIFFERENT PROCEDURES

2.1 Disaggregation of PSHA for ground motion selection

The bridge used for the NLRHA (described in Section 3.1) is located in a region of moderate seismicity according to the maps of the European Seismic Hazard Model 2020 (ESHM20) [13].

As noted earlier, no disaggregation results have been released for most of the locations in Europe yet; they are expected to be published soon [13]. Nevertheless, the M and R outcomes of the disaggregation are parameters important for ground motion selection, e.g. for the calculation of CMS and CMSV. Two disaggregation analyses were carried out using the publicly available input files of the 'classical' probabilistic seismic hazard analysis (PSHA) used for the computation of ESHM20; one for $P|S_a(0.75s) > S_{a,475yr}(0.75s)$ and one for $P|S_a(1s) > S_{a,475yr}(1s)$. T_x = 0.75s and T_y = 1s were selected because they correspond to the natural periods of the predominant modes of the studied bridge in the longitudinal and the transverse direction, respectively. $S_{a,475yr}$ is the S_a value at bedrock for a return period T_r = 475 yr, which is the return period used for the design of the studied bridge according to the upcoming second-generation Eurocode 8 – Part 2 [14] (see Section 3.1). For the disaggregation analyses, the *OpenQuake* software [15] was used, and the results are shown in Fig. 1. For both T = 0.75s and T = 1s, considerable contributions to the seismic hazard are found from a relatively small-magnitude nearby rupture scenario and from a large-magnitude distant scenario.

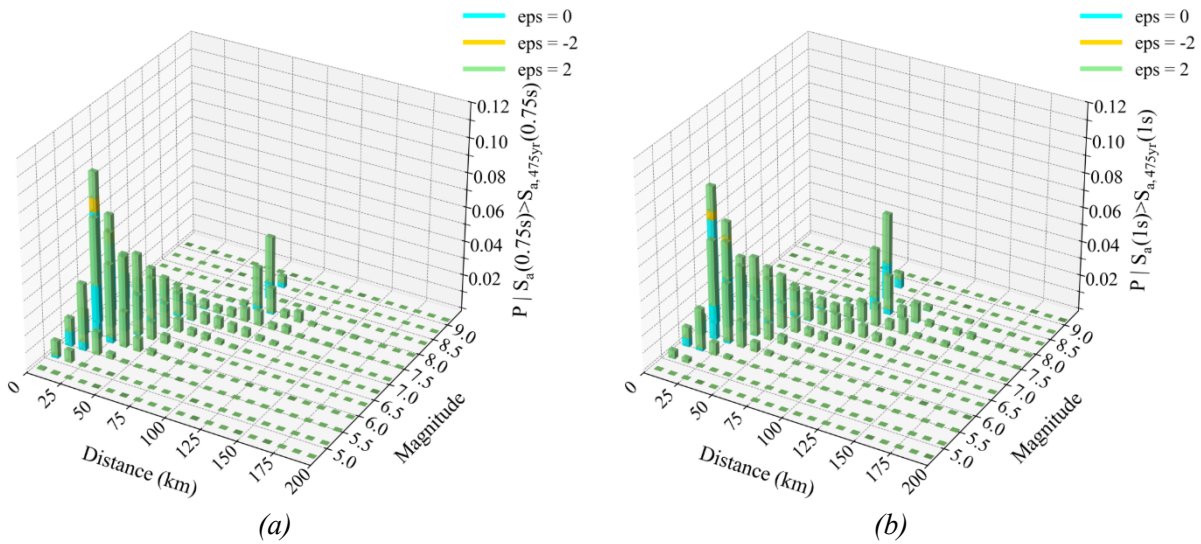

Figure 1: Disaggregation results at the location of the studied bridge for a return period of 475 yr at (a) T = 0.75s and (b) T = 1s

The most commonly used outcome of a disaggregation in engineering applications is a representative effective rupture scenario; here, this scenario is used in two ways: a) to identify the M and R relevant to the return period (T_R) of the seismic actions of interest, as suggested even in the latest seismic codes such as the second-generation Eurocode 8 Part 1-1 [5], and b) to define the input parameters for the ground motion prediction equations (GMPE) used to estimate the expected mean and standard deviation of S_a, which are used in the calculation of

the CMS and the CMSV. The most common options used to identify the effective rupture scenario are the mean and the mode of the disaggregation distribution [3]. In the studied case, the mode of the distribution is (M = 6.2, R= 5km) for both 0.75s and 1s and the mean is (M = 6.5, R = 40 km) for T = 0.75s and (M = 6.7, R = 48) km for T = 1s. Both the mean and the modal rupture scenarios were tried, to compare their effect on the motion selection strategy and, eventually, on the results of the NLRHA.

2.2 Target spectra and causal rupture parameters

The causal rupture parameters, the target spectrum type, and the direction in which the selected ground motions will be applied in the NLRHA are presented in Table 1. Note that soil class C as per Eurocode 8 was considered in all cases. Each set consists of n_{gm} = 7 motions, which is still the minimum allowed by the second-generation Eurocode 8 – Part 1-1.

	M_w	*R (km)*	*Fault type*	*Spectrum type*	*T*(s)*	*Dir.*
CMS(0.75s) – M6.5-R40km	[6.0-7.0]	[30-50]	N[1]+SS[2]	CMS	0.75	X
CMS(1s) – M6.7-R48km	[6.2-7.2]	[38-58]	N+SS	CMS	1.0	Y
CMS – Tarbali & Bradley	NF[3]:[4.8-7.5] DF[4]:[7.5-8.5]	NF:[0-75] DF:[75-200]	NF:N DF:SS	CMS	0.75	X
CMSV(0.75-1s) – M6.6-R44km	[6.0-7.2]	[30-58]	N+SS	CMSV	0.75-1.0	X and Y
UHS – M6.5-R40km	[6.0-7.0]	[30-50]	N+SS	UHS	-	X
UHS – M6.7-R48km	[6.2-7.2]	[38-58]	N+SS	UHS	-	Y
UHS – M6.2-R5km	[5.7-6.7]	[0-20]	N	UHS	-	X
UHS – Tarbali & Bradley	NF:[4.8-7.5] DF:[7.5-8.5]	NF:[0-75] DF:[75-200]	NF:N DF:SS	UHS	-	X
CDS – M6.5-R40km	[6.0-7.0]	[30-50]	N+SS	CDS	-	X
CDS – M6.7-R48km	[6.2-7.2]	[38-58]	N+SS	CDS	-	Y

[1]N: normal fault, [2]SS: striking-slip fault, [3]NF: nearby-fault scenario, [4]DF: distant-fault scenario

Table 1: Causal rupture parameters, target spectrum and bridge direction considered for each set of input ground motions

The used target spectra are UHS, CDS, CMS, and CMSV. The (median) UHS is derived from the input files of PSHA used to calculate ESHM20 for T_r = 475 yr, with the addition of $V_{s,30}$ of the site of interest, adopted from the publicly available site model of the ESHM20 for the Euro-Mediterranean region. CDS is derived from the calculated UHS as per the new Eurocode 8 – Part 1-1 process, which is described in [16]. CMS and CMSV are calculated according to [6] and [8], respectively. Two CMS, one with T* = T_x = 0.75s and one with T* = T_y = 1.0s and a CMSV conditioned to a T* range of [0.75-1.0] s are generated.

In the calculation of CMS, $\rho(T_i)$, the empirically estimated correlation coefficient between $\ln S_a(T^*)$ and $\ln S_a(T_i)$ was obtained from the model of Baker and Jayaram [17], estimated based on the ground motions of the NGA database, most of which had been recorded in the US. Nevertheless, the comparison of the Baker and Jayaram model with models that used data from

other regions, including Europe, showed that $\rho(T_i)$ values are similar for any T* regardless of the specific model used to estimate them [18].

To increase the availability of ground motions, both the NGA-West2 and ESM databases were used. The same rupture scenario parameters shown in Table 1 were employed as search filters in both databases. It is noted that the epicentral distance R was used instead of the Joyner-Boore distance R_{JB} that it is used in the GMPEs employed in our study due to the lack of any R_{JB} data in ESM. The M_w and R tolerances around the disaggregation-based effective rupture scenarios used in the database searches are also shown in Table 1. In most cases, a ±0.5 and a ±10 km ranges were used for M_w and R, respectively, whereas in the 'Tarbali & Bradley' scenarios, the relaxed M-R constraints suggested in [11] were used, with a reasonable modification that helps reducing the computational cost of the ground motion selection algorithm, as described in the following. Namely, the bounds resulting from the suggestions of [11] ended up in a very large number of candidate ground motions. A characteristic example of the relationship between the number of the candidate motions and the number of candidate combinations is given in Fig. 2; it is clarified that when a database of $n_{db} = 50$ motions is used, there are 10^8 possible combinations of $n_{gm} = 7$ motions, while when the database size drops to $n_{db} = 20$, the number of the possible combinations is 7.8×10^3. Additionally, the online databases used in this study can usually return up to a specific maximum number of motions after a user's inquiry. E.g., NGAWest-2 returns up to 100 motions and when the relaxed constraints mentioned above are applied, lots of these motions are often obtained from the same seismic event. Obtaining more than two motions from the same event is usually discouraged (e.g., [5]) because it may lead to biased response estimates, especially when n_{gm} is small.

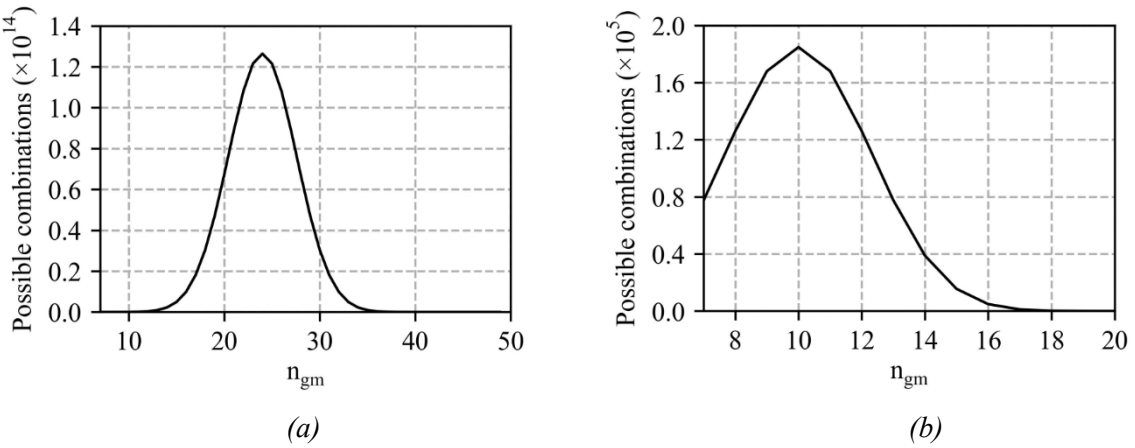

Figure 2: Number of possible combinations as a function of n_{gm} for a database size of (a) $n_{db} = 50$ and (b) $n_{db} = 20$ ground motions

For these reasons, the relaxed M-R constraints defined in [11] are refined here, considering the disaggregation results shown in Fig. 1. The database of the candidate ground motions consists of two M-R bins, each one corresponding to a mode of the disaggregation contribution (see Fig. 1). The rupture mechanism of the faults that contribute to either mode is also taken into account, as shown in Table 1. In this way, the number of the candidate motions in the 'Tarbali & Bradley' CMS and UHS scenarios is reduced to $n_{db} = 31$ motions, resulting in 2.6×10^6 combinations of 7 ground motions. In the other cases, n_{db} varies between 18 and 22.

2.3 In-house developed software for ground motion selection and scaling following the new Eurocode 8 criteria

The decision to merge search results from two different databases, along with the incompatibility of the new Eurocode 8 criteria for motion selection and scaling with the selection tool in either database, led to the development of an in-house program (written in Python). This program enables selection and scaling of motions from a user-defined database, following the relevant recommendations of the new Eurocode 8 – Part 1-1. As most similar programs used in past studies, this software also handles motion selection and scaling as a constrained optimisation problem using the minimisation of the sum of square errors (SSE) between the S_a of the motions and the target spectrum as the objective function [10]. The program is designed to prioritise the selection of a set consisting of unscaled motions over scaled ones and to handle the selection of unscaled and scaled motions differently. For unscaled motions, it performs an exhaustive selection procedure, whereas for scaled motions, it follows a near-optimal, less rigorous, approach similar to the one described in [19], ensuring, in any case, compliance with the quantitative criteria described in Annex D of the new Eurocode 8. The steps involved in the algorithm are summarised below:

Step 1: The user defines the database of the pseudo-acceleration spectra of the n_{db} candidate ground motions after a preliminary screening according to their preferred causal parameter criteria, the target spectrum, the size of the ground motion set that will finally be selected (n_{gm}), and the period range over which the spectrum compatibility will be checked (the $0.2T_1 – 1.5T_1$ range suggested in the new Eurocode 8 is the default option).

Step 2: The motions with 5%-damped response spectra that fall below 50% of the target spectrum in the selected period range are excluded from Steps 3 – 6.

Step 3: All the possible combinations of the spectra of the retained unscaled motions are compiled.

Step 4: The ratios of the average spectrum of the motions of each set to the target spectrum for each considered natural period is calculated. If at least one of these ratios does not fall within the band from 75% to 130%, the respective set is excluded from the following steps.

Step 5: If the average value of the ratios of each set as calculated in Step 4 is not greater than 95% of the respective average value of the target spectrum, the respective set is excluded from the following steps.

Step 6: If the number of the remaining motion sets is $\geq n_{gm}$, the SSE of each set with respect to the target spectrum over the selected period range is calculated. The set with the minimum SSE is the selected set of ground motions and the procedure stops here.

Step 7: If the number of ground motion sets remaining after Step 5 is $< n_{gm}$, the SSE of each motion of the initial user-defined database (Step 1) with respect to the target spectrum is calculated. The motions are ranked according to their respective SSE and only the n_{gm} motions with the smallest SSE are used in the following.

Step 8: The response spectrum of each of the n_{gm} remaining motions is scaled from 0.5 to 2.0 times, which is the band suggested by the new Eurocode 8 – Part 1-1 for geotechnical applications or when highly nonlinear response is anticipated, with a scaling factor increment of 0.01. The scaling factor that minimises the SSE for each ground motion is selected as the optimal scaling factor for the motion. The n_{gm} motions multiplied with their respective optimal scaling factors form the new selected set of scaled ground motions.

Step 9 & Step 10: The checks described in Step 4 and Step 5 are performed on the set of scaled ground motions selected in Step 8. If the set of scaled ground motions satisfies these checks, it is considered the selected set and the procedure stops here.

Step 11: If the set of scaled ground motions does not satisfy the checks of Steps 9 and 10, a different n_{gm} value is assigned by the program. For computational efficiency, the default option is $n_{gm} - 1$ if $n_{gm} < n_{db}/2$, and $n_{gm} + 1$ if $n_{gm} \geq n_{db}/2$ (see Section 2.2 and Fig. 2). The procedure is repeated, starting from Step 2 and using the new n_{gm}. The user may opt for a different n_{gm} or to even stop here without any further iterations.

2.4 Selected ground motion sets

In this section, the 10 sets of ground motions are selected by implementing the algorithm described in Section 2.3. The average spectra of the selected sets for the NLRHA in either direction are shown in Fig. 3. The difficulty in fulfilling all the new Eurocode spectrum matching criteria is evident from the fact that in the 'CMS – Tarbali & Bradley' case, which has the most relaxed causal M-R constraints in this study, there is no set of 7 unscaled motions out of the 31 initially selected in Step 1 of the algorithm that fulfils all the criteria. The only cases where a spectrum compatible set of 7 unscaled motions is identified are 'CMSV(0.75-1s) - M6.6-R44km' and 'UHS – Tarbali & Bradley'; even for them, using a single online database could not result in the selection of a spectrum compatible set of unscaled motions.

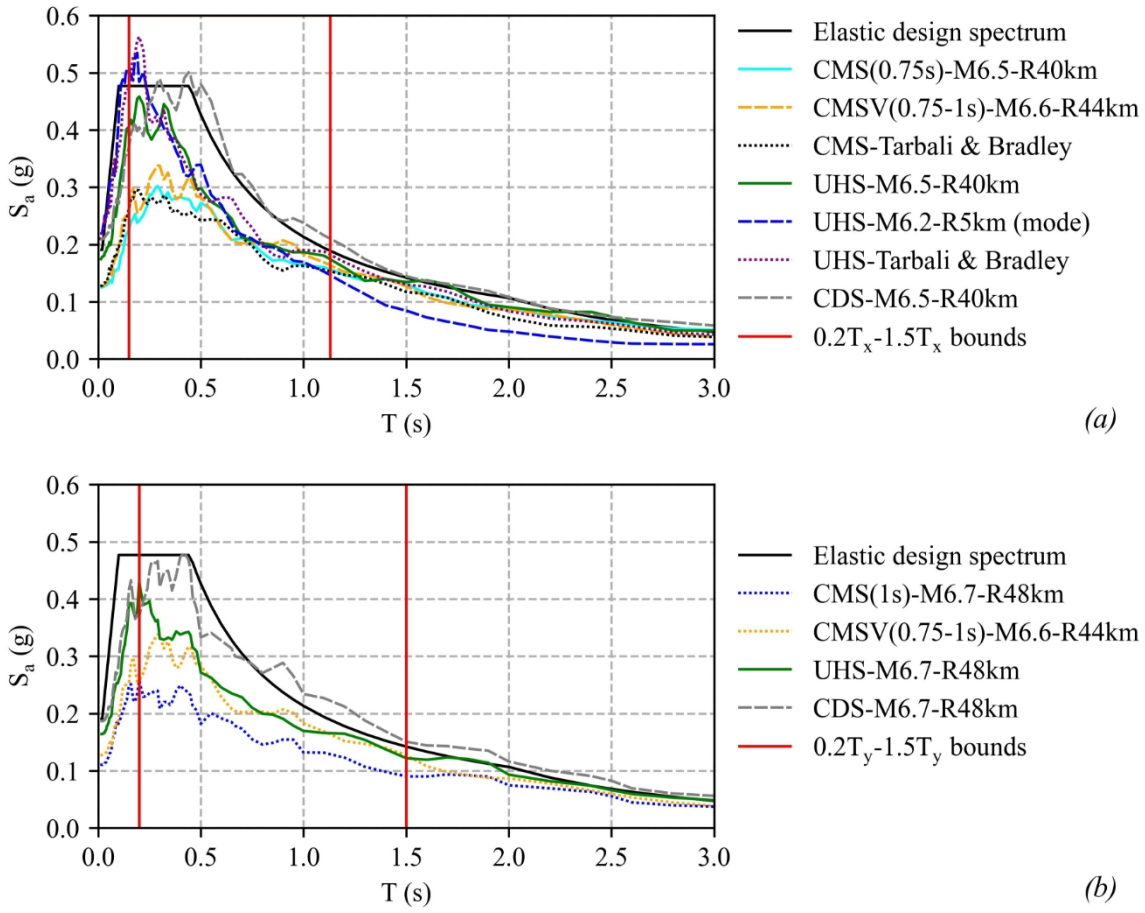

Figure 3: The average spectra of the selected sets of ground motions of the bridge (a) in the X direction and (b) in the Y direction, compared to the elastic design spectrum

3 EFFECT OF GROUND MOTION SELECTION ON NONLINEAR RESPONSE OF BRIDGES

3.1 Case study bridge

The bridge selected to perform the NLRHA is a 100m long, 3-span concrete overpass, located in Northern Greece, designed to the current Eurocodes. Its deck rests on seat-type abutments at its ends through two pairs of elastomeric bearings and it is monolithically connected to its two single-column cylindrical piers, which are 5.9m and 7.9m tall and have a diameter of 1.2m. The nonlinear model of the bridge and more details about its design of the bridge are given in [20]. The characteristics of the first three modes of the bridge are summarised in Table 2.

Mode	*T (s)*	U_X	U_Y	R_Z
1	1.02	-	0.60	0.36
2	0.78	-	0.36	0.61
3	0.75	0.95	-	-

Table 2: Modal participation mass ratios of the three predominant modes of the studied bridge (fixed supports considered)

3.2 Results

The bridge is subjected to NLRHA in *OpenSeesPy* [21] using the selected sets as input motions. To obtain more clear results that are easier to compare, analyses were carried out separately in each direction. The only set of motions that was used in both directions is the 'CMSV(0.75-1s) - M6.6-R44km' since the used CMSV is conditioned on both T_x = 0.75s and T_y = 1s. For each set of motions, the average of the maximum deck displacement $\delta_{d,max}$ from the 7 input motions was calculated, consistently with Eurocode 8 requirement. Due to the different modal behaviour of the bridge in its two directions, the maximum displacements are recorded at different locations of the deck when NLRHA is performed in either direction. Namely, in the X direction, where the predominant mode is translational, $\delta_{d,max}$ is recorded in the middle of the deck, whereas in the Y direction, where the torsional mode contribution is significant (Table 2), $\delta_{d,max}$ is recorded at the end of the deck that is closer to the tallest pier.

The resulting average $\delta_{d,max}$ for each set of ground motions is shown in Table 3 in an ascending order. It is clear that matching to CDS is the most conservative option, which leads to about 50% increase in the response estimates in both directions compared to the UHS. The relaxation of M-R constraints leads to very small differences compared to a selection based on narrower M-R ranges, although the latter do not correspond strictly to the disaggregation results of Fig. 2. Comparing the NLRHA results of the various target spectrum types in the Y direction, it seems that CMS results in significantly smaller displacements than UHS and CMSV, likely because it is conditioned to first mode only, which has a 60% modal mass participation ratio. Instead, the conditioning period range for CMSV is 0.75-1s, which includes the natural period of the significant second mode as well.

X direction		*Y direction*	
	$\delta_{d,max}$ (m)		$\delta_{d,max}$ (m)
CMS – Tarbali & Bradley	0.026	CMS(1s) – M6.7-R48km	0.049
CMS(0.75s) – M6.5-R40km	0.027	CMSV(0.75-1s) - M6.6-R44km	0.064
CMSV(0.75-1s) – M6.6-R44km	0.029	UHS – M6.7-R48km	0.069
UHS – M6.2-R5km	0.030	DS – M6.7-R48km	0.099
UHS – M6.5-R40km	0.032		
UHS – Tarbali & Bradley	0.033		
DS – M6.5-R40km	0.040		

Table 3: Average $\delta_{d,max}$ for each set of ground motions

4 CONCLUSIONS AND RECOMMENDATIONS

This study examined the impact of common ground motion selection strategies on the nonlinear seismic response of bridges and introduced a ground motion selection tool aligned with the provisions of the new Eurocode 8 – Part 1-1. The in-house developed tool efficiently produces spectrum-compatible sets of unscaled or, if necessary, scaled ground motions using a user-defined target spectrum without relying on sophisticated but computationally demanding algorithms. To avoid excessive computational cost, if scaled motions are required, a near-optimal set is selected by optimising the scaling factors of individual ground motions that meet the code criteria. However, for cases requiring a large number of ground motions (e.g., for uncertainty quantification), more advanced selection algorithms may be preferable.

A key conclusion of this study is that the effect of the causal rupture parameters is not critical, at least in the case of overpasses like the one studied, provided that the selected motion set matches the target spectrum according to the stringent criteria adopted by most modern seismic codes. This outcome is consistent with prior studies, such as [11]. These stringent criteria have two important consequences: first, as clearly seen in the results of the case study, they make the spectrum type arguably the most critical factor in the definition of the seismic action avoiding dependence on the causal parameters, which are usually defined in a subjective way, and second, they hinder motion selection from a single online ground motion database (among those currently available). A solution could be the concurrent use of multiple databases; however, the incompatibility between the various databases makes it a challenging task that can be faced at the moment only with software, such as the one developed in the present study. Relaxed causal rupture parameter constraints could be an alternative, but in several databases, there is a maximum number of motions that can be selected at every search, without ensuring their compliance to the relevant code criteria. To overcome this issue, the preliminary screening of motions in a database could start with tighter causal parameter bounds, which are incrementally relaxed until a set with of adequate ground motions is obtained.

The comparison of the effect of various target spectra on the NLRHA results for the case study bridge also showed some of their advantages and deficiencies. The elastic design spectrum, while readily available to practising engineers, is overly conservative for assessment since it leads to an overestimation of the response. Although more realistic, CMS should be used cautiously since it sometimes leads to underestimation of higher mode contributions, unless multiple CMS are used. The CMSV seems to solve these issues, although its calculation is much more laborious than the usually available UHS, while if CMSV is conditioned to a relatively wide period range, UHS and CMSV may lead to close results.

ACKNOWLEDGEMENTS

The authors gratefully acknowledge the financial support by Khalifa University, Abu Dhabi [research project reference number: RIG-2023-006, Principal Investigator: A. Kappos]. The insight gained by discussions of some aspects of this study with Dr. L. Danciu (ETH Zurich) and Prof. K. Pitilakis (Aristotle University of Thessaloniki) is gratefully acknowledged.

REFERENCES

[1] T. D. Ancheta *et al.*, "NGA-West2 Database," *Earthquake Spectra*, vol. 30, no. 3, pp. 989–1005, 2014

[2] S. Sgobba *et al.*, "REXELweb: A tool for selection of ground-motion records from the Engineering Strong Motion database (ESM)," in *Earthquake Geotechnical Engineering for Protection and Development of Environment and Constructions*, CRC Press, 2019, pp. 4947–4953.

[3] J. Baker, B. Bradley, and P. Stafford, *Seismic Hazard and Risk Analysis*. Cambridge: Cambridge University Press, 2021.

[4] M. Georgioudakis and M. Fragiadakis, "Selection and Scaling of Ground Motions Using Multicriteria Optimization," *Journal of Structural Engineering*, vol. 146, no. 11, p. 04020241, 2020.

[5] CEN, "Eurocode 8 - Design of structures for earthquake resistance - Part 1-1: General rules and seismic action. Technical Committee 250, Sub-Committee 8 (draft)," Brussels, 2024.

[6] J. W. Baker and C. Allin Cornell, "Spectral shape, epsilon and record selection," *Earthquake Engineering & Structural Dynamics*, vol. 35, no. 9, pp. 1077–1095, 2006.

[7] T. Lin, S. C. Harmsen, J. W. Baker, and N. Luco, "Conditional Spectrum Computation Incorporating Multiple Causal Earthquakes and Ground□Motion Prediction Models," *Bulletin of the Seismological Society of America*, vol. 103, no. 2A, pp. 1103–1116, 2013.

[8] T. Kishida, "Conditional Mean Spectra Given a Vector of Spectral Accelerations at Multiple Periods," *Earthquake Spectra*, vol. 33, no. 2, pp. 469–479, 2017.

[9] CEN, "Eurocode 8: Design of Structures for Earthquake Resistance–Part 2: Bridges," Brussels, BE, 2005.

[10] D. Caicedo, S. Karimzadeh, V. Bernardo, and P. B. Lourenço, "Selection and Scaling Approaches of Earthquake Time-Series for Structural Engineering Applications: A State-of-the-Art Review," *Archives of Computational Methods in Engineering*, vol. 31, no. 3, pp. 1475–1505, 2024.

[11] K. Tarbali and B. A. Bradley, "The effect of causal parameter bounds in PSHA-based ground motion selection," *Earthquake Engineering & Structural Dynamics*, vol. 45, no. 9, pp. 1515–1535, 2016.

[12] V. Manfredi, A. Masi, A. G. Özcebe, R. Paolucci, and C. Smerzini, "Selection and spectral matching of recorded ground motions for seismic fragility analyses," *Bulletin of Earthquake Engineering*, vol. 20, no. 10, pp. 4961–4987, 2022.

[13] L. Danciu *et al.*, "The 2020 update of the European Seismic Hazard Model: Model Overview. EFEHR Technical Report 001, v1. 0.0," 2021.

[14] CEN, "Eurocode 8 — Design of structures for earthquake resistance — Part 2: bridges. Technical Committee 250, Sub-Committee 8 (draft)," Brussels, BE, 2024.

[15] M. Pagani *et al.*, "OpenQuake engine: An open hazard (and risk) software for the global earthquake model," *Seismological Research Letters*, vol. 85, no. 3, pp. 692–702, 2014.

[16] P. Labbé and R. Paolucci, "Developments Relating to Seismic Action in the Eurocode 8 of Next Generation," in *Progresses in European Earthquake Engineering and*

Seismology, R. Vacareanu and C. Ionescu, Eds., Cham: Springer International Publishing, 2022, pp. 26–46.

[17] J. W. Baker and N. Jayaram, "Correlation of Spectral Acceleration Values from NGA Ground Motion Models," *Earthquake Spectra*, vol. 24, no. 1, pp. 299–317, Feb. 2008, doi: 10.1193/1.2857544.

[18] J. W. Baker and B. A. Bradley, "Intensity Measure Correlations Observed in the NGA-West2 Database, and Dependence of Correlations on Rupture and Site Parameters," *Earthquake Spectra*, vol. 33, no. 1, pp. 145–156, 2017.

[19] R. Youngs, M. Power, G. Wang, F. Makdisi, and C. C. Chin, "Design ground motion library (DGML)–tool for selecting time history records for specific engineering applications," in *SMIP07 Seminar on Utilization of Strong-Motion Data*, California Geological Survey Sacramento, CA, 2007, pp. 109–110.

[20] I. G. Mikes and A. J. Kappos, "Modelling of the post-peak response of abutment-backfill systems: a new hysteretic model for OpenSees," *Bulletin of Earthquake Engineering*, vol. 22, no. 5, pp. 2723–2737, 2024.

[21] M. Zhu, F. McKenna, and M. H. Scott, "OpenSeesPy: Python library for the OpenSees finite element framework," *SoftwareX*, vol. 7, pp. 6–11, 2018.